



University of Dundee

Structural and Atropisomeric Factors Governing the Selectivity of Pyrimido-benzodiazipinones as Inhibitors of Kinases and Bromodomains

Wang, Jinhua; Erazo, Tatiana; Ferguson, Fleur M.; Buckley, Dennis L.; Gomez, Nestor; Muñoz-Guardiola, Pau

Published in:
ACS Chemical Biology

DOI:
[10.1021/acscchembio.7b00638](https://doi.org/10.1021/acscchembio.7b00638)

Publication date:
2018

Document Version
Peer reviewed version

[Link to publication in Discovery Research Portal](#)

Citation for published version (APA):

Wang, J., Erazo, T., Ferguson, F. M., Buckley, D. L., Gomez, N., Muñoz-Guardiola, P., ... Gray, N. S. (2018). Structural and Atropisomeric Factors Governing the Selectivity of Pyrimido-benzodiazipinones as Inhibitors of Kinases and Bromodomains. *ACS Chemical Biology*, 13(9), 2438-2448. <https://doi.org/10.1021/acscchembio.7b00638>

General rights

Copyright and moral rights for the publications made accessible in Discovery Research Portal are retained by the authors and/or other copyright owners and it is a condition of accessing publications that users recognise and abide by the legal requirements associated with these rights.

- Users may download and print one copy of any publication from Discovery Research Portal for the purpose of private study or research.
- You may not further distribute the material or use it for any profit-making activity or commercial gain.
- You may freely distribute the URL identifying the publication in the public portal.

Take down policy

If you believe that this document breaches copyright please contact us providing details, and we will remove access to the work immediately and investigate your claim.

Structural and atropisomeric factors governing the selectivity profile of pyrimido-benzodiazepinones as inhibitors of kinases and bromodomains

Jinhua Wang^{1,2}, Tatiana Erazo³, Fleur M. Ferguson^{1,2}, Dennis L. Buckley⁴, Nestor Gomez³, Pau Muñoz-Guardiola³, Nora Dieguez-Martinez³, Xianming Deng^{1,2}, Ming-Feng Hao¹, Walter Massefski¹, Oleg Fedorov⁵, Nana Kwaku Offei-Addo⁴, Amy DiBona⁶, Kelly Becht⁶, Nam Doo Kim⁷, Michael R. McKeown⁴, Justin M. Roberts⁴, Jinwei Zhang⁸, Taobo Sim⁹, Dario R. Alessi⁸, James E. Bradner⁴, Jose M. Lizcano³, Stephen C. Blacklow^{1,2}, Jun Qi⁴, Xiang Xu^{1,2*}, Nathanael S. Gray^{1,2*}

1. Department of Cancer Biology, Dana-Farber Cancer Institute, Boston, MA 02215, USA.
2. Department of Biological Chemistry & Molecular Pharmacology, Harvard Medical School, Boston, MA 02115, USA.
3. Institut de Neurociències, Departament de Bioquímica i Biologia Molecular, Facultat de Medicina. Universitat Autònoma de Barcelona, E-08193 Barcelona, Spain.
4. Department of Medical Oncology, Dana-Farber Cancer Institute, Harvard Medical School, Boston, Massachusetts, USA.
5. Structural Genomics Consortium and Target Discovery Institute, Nuffield Department of Clinical Medicine, University of Oxford, Oxford, UK.
6. Department of Pathology, Brigham and Women's Hospital, Harvard Medical School, Boston, Massachusetts, USA.
7. NDBio Therapeutics Inc., 32 Songdogwahak-ro, Yeonsu-gu, Incheon 21984, Republic of Korea
8. MRC Protein Phosphorylation and Ubiquitination Unit, College of Life Sciences, University of Dundee, Dow Street, Dundee DD1 5EH, Scotland, United Kingdom.
9. Chemical Kinomics Research Center, Korea Institute of Science and Technology, Seoul, Korea and KU-KIST Graduate School of Converging Science and Technology, Seoul, Korea.

ABSTRACT: Bromodomains have been pursued intensively over the past several years as emerging targets for the development of anti-cancer and anti-inflammatory agents. It has recently been shown that some kinase inhibitors are able to potently inhibit the bromodomains of BRD4. The clinical activity of PLK inhibitor BI-2536 and JAK2-FLT3 inhibitor TG101348 have been attributed to this unexpected poly-pharmacology, indicating that dual-kinase/bromodomain activity may be advantageous in a therapeutic context. However, for target validation and biological investigation, a more selective target profile is desired. Here we report that benzo[e]pyrimido-[5,4-b]diazepine-6(11H)-ones, versatile ATP-site directed kinase pharmacophores utilized in the development of inhibitors of multiple kinases including a number of previously reported kinase chemical probes, are also capable of exhibiting potent BRD4-dependent pharmacology. Using a dual kinase-bromodomain inhibitor of the kinase domains of ERK5 and LRRK2, and the bromodomain of BRD4 as a case study, we define the structure-activity relationships required to achieve dual kinase/BRD4 activity as well as how to direct selectivity towards inhibition of either ERK5 or BRD4. This effort resulted in identification of one of the first reported kinase-selective chemical probes for ERK5 (**JWG-071**), a BET selective inhibitor (**JWG-115**), and additional inhibitors with rationally designed polypharmacology (**JWG-047**, **JWG-069**). Co-crystallography of seven representative inhibitors with the first bromodomain of BRD4 demonstrate that distinct atropisomeric conformers recognize the kinase ATP-site and the BRD4 acetyl lysine binding site, and this conformational preferences is supported by rigid docking studies.

INTRODUCTION

BRD4 is a critical transcription co-activator protein that possesses two druggable acetyl lysine binding domains (bromodomains) targeting the protein to chromatin by binding acetylated histones.¹ BRD4 is a master regulatory elongation factor, influencing function of CDK9², the kinase activity of which is essential to phosphorylate RNA Polymerase II to initiate transcription,³⁻⁵ and aberrant activity of BRD4 contrib-

utes to deregulated transcription, a hallmark of many cancers.⁶⁻⁸ BRD4 has been actively pursued as an oncology drug target with at least six compounds that target the acetyl lysine binding pocket currently under clinical investigation.⁹ These selective BET inhibitors have demonstrated phenotypic effects against a broad range of cancer cell lines and in models of inflammation, atherosclerosis and male fertility.

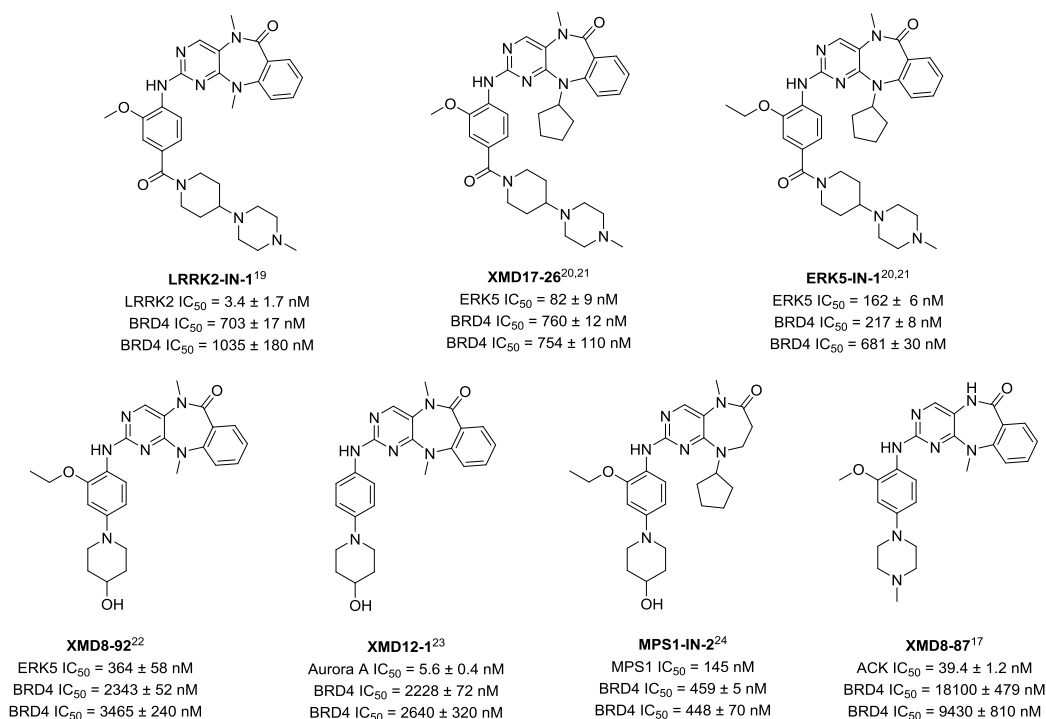


Figure 1. BRD4 (BD1) inhibition of published kinase chemical probes. Kinase IC₅₀s are as previously published in references. BRD4 IC₅₀ values were measured by AlphaScreen™ binding assay and reported as the average of 2 replicates ± SE (conducted in Dana-Farber Cancer Institute, top data) and as the average of 4 replicates ± SD (conducted in University of Oxford, bottom data). (+)-JQ1 IC₅₀s are 64 nM and 120 nM respectively.

Synergy between BRD4 inhibition and a multitude of kinase inhibitors has also been identified in cancer (*e.g.* with FLT3-TKI¹⁰, rapamycin¹¹ and CX-4945¹²), providing a rationale for development of therapeutics with potent dual BRD4-kinase activity.

Recently several groups have made the surprising discovery that many ATP-competitive kinase inhibitors can also bind potently to the acetyl-lysine binding domain of BRD4.^{13,14} Kinase inhibitors based on at least 10 different scaffolds have been shown to inhibit the BRD4 bromodomains. The clinical activity of the PLK inhibitor BI-2536 and the JAK2-FLT3 inhibitor TG101348 have been attributed to this unexpected poly-pharmacology, indicating that in a therapeutic context dual kinase-bromodomain activity may be desirable.

However, due to its ubiquitous expression and central importance to the regulation of transcription, uncharacterized off-target BRD4 activity in chemical probes is undesirable, as it complicates the connection between the target and any phenotypes observed. Characterization of the BRD4 activity of classical kinase inhibitor scaffolds, and the trends governing the selectivity profile are important for unraveling the pharmacologically relevant targets for these compounds. To this end, extensive work has been invested in characterizing the factors governing the PLK and BRD4 activity of BI-2536 analogs based on a privileged ATP-site targeting pyrido[2,3-d]pyrimidine core.^{15,16}

Here we characterize the SAR trends and structural basis for the kinase and bromodomain activity profile of the related benzo[e]pyrimido-[5,4-b]diazepine-6(1H)-ones and use these rules to generate selective chemical probes for ERK5/LRRK2 and BRD4, and to develop rationally designed dual kinase (ERK5/LRRK2)-BRD4 inhibitors. We also observed two distinct conformers exclusively recognize the kinase ATP-site

and the BRD4 acetyl lysine-binding site and analyzed the interconversion rate for conformers with large substituents.

RESULTS AND DISCUSSION

ERK5 inhibitors XMD11-50 (LRRK2-IN-1) and XMD17-26 are dual kinase-bromodomain inhibitors.

Based on the privileged nature of the pyrido[2,3-d]pyrimidine core of BI-2536 as an ATP-site targeting scaffold, we had built combinatorial libraries of analogs with a benzo[e]pyrimido-[5,4-b]diazepine-6(1H)-one scaffold for use in kinase inhibitor projects, resulting in the discovery of multiple kinase inhibitor tool compounds (Figure 1).¹⁷ In order to test if this series also inhibits BRD4, analogous to BI-2536, we performed a BRD4 AlphaScreen assay of our kinase-biased chemical library (data not shown).¹⁸ Many diazepinones were found to be active. Importantly some hits from this screen are published “selective” kinase chemical probes,¹⁹⁻²⁴ and therefore this result provides valuable insight into their observed pharmacology^{25,26} (Figure 1). These molecules represent a new class of dual kinase-bromodomain inhibitors.

We chose to investigate the structure activity relationship (SAR) of this scaffold against both ERK5/LRRK2 and BRD4, using BRD4 hit compounds XMD11-50 (LRRK2-IN-1) and XMD17-26 (published as an ERK5 inhibitor) as chemical starting points, aiming to develop a selective ERK5 inhibitor. This was motivated by the dual kinase-bromodomain inhibition profile of the compounds (Figure 1), the lack of availability of a selective ERK5 chemical probe, the poorly characterized biological function of ERK5, and the potential of ERK5 as a cancer drug target. Specifically, the MEK5/ERK5 pathway has been reported to be activated and/or overexpressed during tumor development, metastasis and tumor angiogenesis.²⁷⁻²⁹

Table 1. Evaluation of initial BRD4 hits.

Compound ID	IC ₅₀ (nM) ^a	IC ₅₀ (nM) ^b	K _d (nM) ^c	ΔTm (°C) ^d
XMD11-50 (LRRK2-IN-1)	703 ± 17	1040 ± 180	192 ± 28	2.1 ± 0.37
XMD17-26	760 ± 12	754 ± 110	156 ± 12	4.1 ± 0.24
(+)-JQ1	64	120	49.0 ± 2.4*	10.1 ± 0.11

^aIC₅₀ values were measured by AlphaScreen™ binding assay and reported as the average of 2 replicates ± SE. Experiments were conducted in Dana-Farber Cancer Institute. ^bIC₅₀ values were measured by AlphaScreen™ binding assay and reported as the average of 4 replicates ± SD. Experiments were conducted in University of Oxford. ^cK_d values were measured by ITC and reported as the average of 4 replicates ± SD. ^dΔTm values were measured by DSF and reported as the average of 3 replicates ± SD. *The JQ1 K_d value is from a previous publication.

We began by confirming the BRD4 activity of the hit kinase inhibitors using isothermal titration calorimetry (ITC) and differential scanning fluorimetry (DSF) (**Table 1**), using (+)-JQ1 as a BRD4 positive control. These data were in good agreement with IC₅₀ values measured by AlphaScreen. Both compounds show comparable potency to other well characterized dual kinase/bromodomain inhibitors.^{13,14}

To understand how these compounds bind to BRD4-BD1, we determined X-ray co-crystal structures of BRD4-BD1 with both XMD11-50 and XMD17-26 to 1.2 Å and 1.6 Å resolution respectively. (**Figure 2A, 2B** and **Supplemental Table 1**). Both XMD11-50 and XMD17-26 were clearly defined in the electron density maps and bound in the acetyl lysine binding pocket (**Supplemental Figure 3**). The core of the benz[e]pyrimido-[5,4-b]diazepine-6(11H)-one scaffold is buried deeply in the pocket and mediates most direct interactions with the protein (**Figure 2A, 2B**). It forms two hydrogen bonds directly with the bromodomain, one with the side chain of conserved Asn140, the other with the carbonyl oxygen of Pro82. The N-methyl amide group in the diazepamone ring fills a hydrophobic cavity in a manner analogous to N-acetyl group of an acetylated lysine residue.³⁰ Structural waters are usually conserved and mediate a ligand-bromodomain interaction. In the XMD11-50 structure, there are three key structural waters forming hydrogen bonds with the ligand directly, and bridging hydrogen-bond interactions with the side chains of Gln85 and

Tyr97, the carbonyl oxygens of Pro86 and Gln85, and main chain nitrogen of Asn88 (**Figure 2A**). In addition, the methoxyphenyl moiety of the aniline tail forms a hydrophobic interaction with the WPF shelf in the ZA loop. The rest of the ligand tail consisting of the methyl-4-piperidine-4-yl piperazine moiety is solvent exposed, which suggests that it is not essential for ligand-protein recognition. The structure of XMD17-26 shares the same core interactions observed in the XMD11-50 structure (**Figure 2B**). In addition, the WPF shelf forms a hydrophobic interaction with the cyclopentyl R₁ substituent of XMD17-26. The more bulky cyclopentyl substituent also causes a shift in the conformation of the tricyclic ring system. As a result, different angles between the planes of the scaffold are observed for the two compounds in the X-ray structures (**Figure 2C**).

Modulating selectivity for BRD4, ERK5 and LRRK2.

We initiated our studies with a systematic structure-activity relationship analysis of the R₁ substitution (**Table 2**). The R₁ group influences the conformation of the 7-membered diazepamone ring and mediates steric and hydrophobic interactions with BRD4. Thus, we anticipated that R₁ substitutions would affect BRD4 activity and result in different selectivity profiles against BRD4, ERK5 and LRRK2. The newly synthesized compounds were tested for their ability to inhibit ERK5 and LRRK2 *in vitro* kinase activities, ERK5 cellular activity in human HeLa cells, BRD4-BD1 binding affinity and BRD4 cellular activity in the BRD4-dependant 797 NUT-midline carcinoma cells which harbors a BRD4-NUT fusion oncogene.³¹ Addition of progressively larger alkyl substituents at R₁, from methyl (**XMD11-50**) to sec-butyl (**JWG-071**) resulted in gradually reduced binding affinity for BRD4 and LRRK2, but had almost no effect on ERK5 inhibition, which may be due to steric clashes with the αC-helix of BRD4, indicating this position is a crucial hotspot for dialing out bromodomain targets while maintaining ERK5 kinase activity. All attempts to synthesize 3-pentyl substituted analogs to explore the effect of larger substituents at R₁ failed, possibly due to steric hindrance. Having identified a kinase class-selective compound, the kinome wide selectivity of **JWG-071** was assessed using the KinomeScan methodology (DiscoverX) across a panel of 468 human kinases at a concentration of 1 μM. Only two kinases, ERK5 and DCAMKL2, were hits in this assay (Ambit scores of less than 10%, **Supplemental Figure 4** and Supplemental data). This off-target kinase activi-

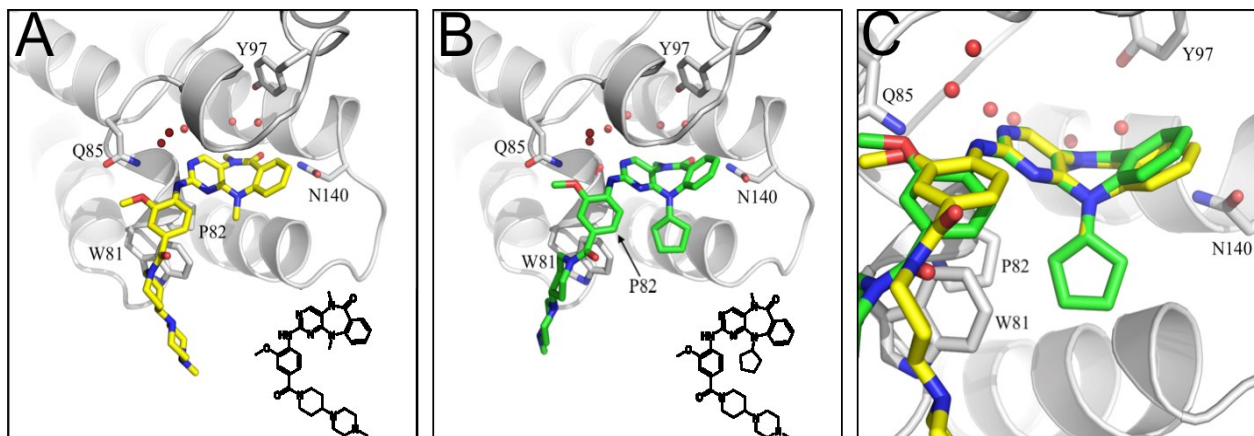
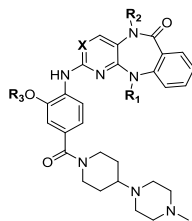


Figure 2. (A) X-ray structure of **XMD11-50** bound to BRD4-BD1. (B) X-ray structure of **XMD17-26** bound to BRD4-BD1. (C) Overlay of the two compounds highlighting the different angular configuration of the diazepamone ring system.

Table 2. Activity profile of inhibitors with diazepinone scaffold

Compound ID	R ₁	R ₂	R ₃	X	Biochemical IC ₅₀ (BRD4, μM) ^a	Biochemical IC ₅₀ (BRD4, μM) ^b	Enzymatic IC ₅₀ (ERK5, μM) ^c	Enzymatic IC ₅₀ (LRRK2, μM) ^d	Viability IC ₅₀ (BRD4, μM) ^e	Cellular EC ₅₀ (ERK5, μM) ^f	Inhibitor classification ^g	Co-crystal (pdb number)
XMD11-50 (LRRK2-IN-1)	Me	Me	Me	N	0.703 ± 0.017	1.04 ± 0.18	0.114 ± 0.011	0.0034 ± 0.0017	1.989 ± 0.299	0.16 ± 0.04	BRD4/LRRK2	Roco4 (4YZM) ³² BRD4 (5WA5)
JWG-048	Et	Me	Me	N	1.33 ± 0.05	2.41 ± 0.23	0.173 ± 0.037	0.0044 ± 0.0005	2.625 ± 0.540	0.022 ± 0.004	LRRK2	BRD4 (5W55)
JWG-046	<i>i</i> -Pr	Me	Me	N	4.59 ± 0.14	5.14 ± 0.59	0.125 ± 0.026	0.054 ± 0.004	ND	0.014 ± 0.004	ERK5/LRRK2	BRD4 (6CD4)
JWG-071	<i>s</i> -Bu	Me	Me	N	5.42 ± 0.18	6.31 ± 1.93	0.088 ± 0.005	0.109 ± 0.014	>10	0.020 ± 0.003	ERK5/LRRK2	BRD4 (6CJ1)
JWG-069	cyclobutyl	Me	Me	N	0.201 ± 0.007	0.41 ± 0.01	0.075 ± 0.009	0.021 ± 0.001	0.116 ± 0.001	0.019 ± 0.005	BRD4/ERK5/LRRK2	BRD4 (6CIY)
XMD17-26	cyclopentyl	Me	Me	N	0.760 ± 0.012	0.75 ± 0.11	0.082 ± 0.009	0.095 ± 0.010	0.664 ± 0.014	0.08 ± 0.02	BRD4/ERK5/LRRK2	ERK5 (4B99) ²¹ BRD4 (5CD5)
JWG-112	<i>s</i> -Bu	H	Me	N	25.7 ± 1.8	>40	>10	1.59 ± 0.37	ND	ND	No activity	
JWG-049	<i>i</i> -Pr	Me	Et	N	2.50 ± 0.07	3.53 ± 0.82	0.069 ± 0.007	0.114 ± 0.011	ND	0.025 ± 0.007	ERK5/LRRK2	
JWG-114	<i>i</i> -Pr	Me	<i>i</i> -Pr	N	0.862 ± 0.065	1.08 ± 0.13	0.421 ± 0.007	0.235 ± 0.034	ND	ND	BRD4/weak LRRK2	
XMD17-109 (ERK5-IN-1)	cyclopentyl	Me	Et	N	0.217 ± 0.008	0.68 ± 0.03	0.162 ± 0.006	0.171 ± 0.030	ND	0.09 ± 0.03	BRD4/ERK5/LRRK2	
JWG-047	cyclopentyl	Me	<i>i</i> -Pr	N	0.135 ± 0.004	0.30 ± 0.05	0.160 ± 0.008	0.296 ± 0.031	0.465 ± 0.012	0.032 ± 0.009	BRD4/ERK5/LRRK2	BRD4 (6CIS)
AX15836	SO ₂ Me	Me	Et	N	>100	>40	0.012 ± 0.002	0.942 ± 0.569	ND	0.036 ± 0.004	ERK5	
DFCI-2-208	Me	Me	Me	C	5.21 ± 0.14	4.64 ± 0.65	>10	>10	ND	ND	No activity	
JWG-115	cyclopentyl	Me	<i>i</i> -Pr	C	1.08 ± 0.05	1.10 ± 0.05	>10	> 3.3	ND	ND	BRD4 (weak)	
(+)-JQ-1					0.064	0.12	>10	>10	0.228	ND	BRD4	

^aIC₅₀ values were measured by AlphaScreen™ binding assay and reported as the average of 2 replicates ± SE. Experiments were conducted in Dana-Farber Cancer Institute. ^bIC₅₀ values were measured by AlphaScreen™ binding assay and reported as the average of 4 replicates ± SD. Experiments were conducted in University of Oxford. ^cIC₅₀ values were measured by in vitro assay and reported as the average of 2 replicates ± SD. ^dIC₅₀ values were measured using Adapta assay format (ThermoFisher Scientific) and reported as the average of 2 replicates ± SD. ^eIC₅₀ were determined in 797 NUT-midline carcinoma cells by cell numbers using Cell Titer Glo and reported as the average of 3 replicates ± SD. ^fEC₅₀ values were measured by EGF-stimulated autophosphorylation of ERK5 in HeLa cells and reported as the average of 2 replicates ± SD. ^gConsidering that weak BET bromodomain inhibition has been shown to result in phenotypic responses, a BRD4 activity within 20 fold of JQ1 was defined as BET active. 0.2 μM was chosen as the threshold for kinase activity. A 10-fold activity difference among kinases was considered selective.

ty was confirmed in biochemical enzyme assays, where JWG-071 showed little selectivity for ERK5 relative to LRRK2 and DCAMKL2 *in vitro* (1.2 and 2.5 folds respectively). Compared to the previously published ERK5 tool compound **XMD17-109 (ERK5-IN-1)**, **JWG-071** has 2-fold improved ERK5 activity, and 10-fold improved BRD4 selectivity. Overall, these data show that **JWG-071** will be a much-needed chemical probe for deconvoluting ERK5 and BRD4 pharmacology.

Surprisingly, the cyclobutyl and cyclopentyl R₁ substituted compounds **JWG-069** and **XMD17-26** exhibited strong binding to BRD4. These cyclic substitutions were also well tolerated by ERK5 and LRRK2, indicating that these are optimal R₁ groups for achieving BRD/Kinase polypharmacology.

The activities of corresponding analogs with 2-methoxy-4-(4-methylpiperazin-1-yl) aniline tails against ERK5, LRRK2

and BRD4 displayed a similar trend, although with slightly lower BRD4 binding, indicating that the activity difference is mainly due to the changes to interactions with the R₁ substituent and the benzo[e]pyrimido-[5,4-b]diazepine-6(1H)-one core structure (**Supplemental Table 2**).

In order to gain a structural understanding of this piece of the SAR, we determined crystal structures of BRD4 with the R₁ analogs (**Table 2**, entries 2-5, **Supplemental Table 1**), and compared them to the structures with **XMD11-50** and **XMD17-26**. The binding mode and key interaction with Asn140 is conserved among all analogs. Alkyl substitutions at the R₁ position introduce additional steric restrictions, changing the angular configuration of the “butterfly-shaped” tricyclic core as seen in the structure of XMD17-26 (**Figure 3A**).

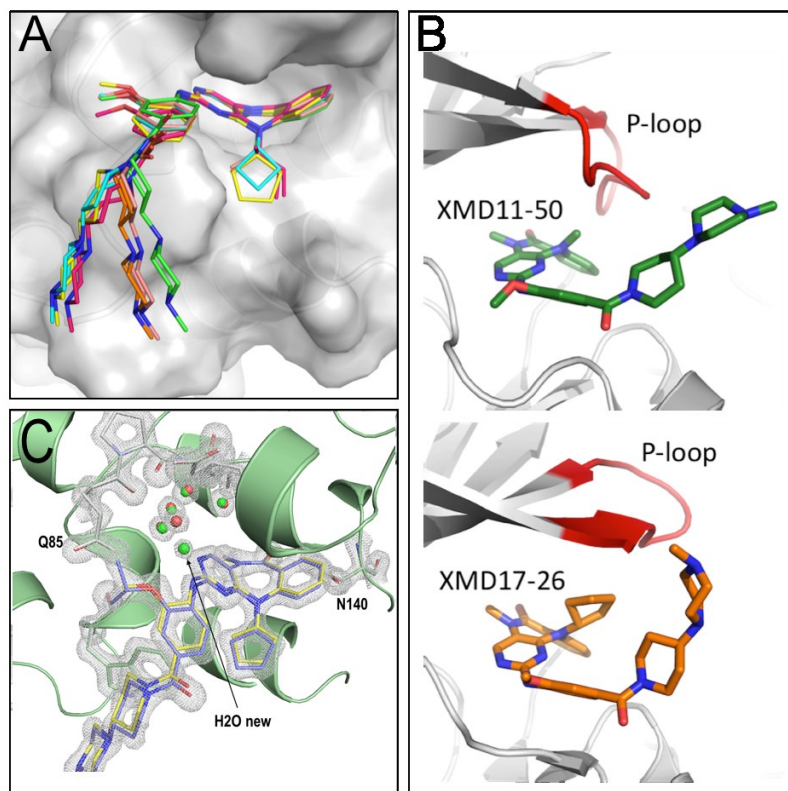


Figure 3. (A) Overlay of structures of **XMD11-50** (green), **JWG-048** (salmon), **JWG-046** (orange), **JWG-071** (pink), **JWG-069** (cyan) and **XMD17-26** (yellow) highlighting the different curvature of the diazopinone ring system and deviation of the tail. (B) Overlay of Roco4/**XMD11-50** (pdb code 4YZM, top), and ERK5/**XMD17-26** (pdb code 4B99, bottom), crystal structure reveal differences in P-loop (red) conformation and explain observed R_2 SAR. (C) Overlay of **JWG-047** and **XMD17-26** in complex with BRD4-BD1 reveal differences in local interactions and the presence of a new water molecule in the **JWG-047** complex.

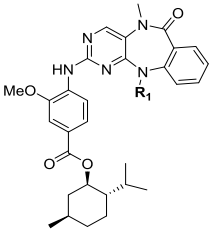
Since co-crystal structures of **XMD17-26** with ERK5 kinase (PDB: 4B99)²¹ and **XMD11-50** with Roco4 kinase (*Dictyostelium disco* homolog of LRRK2, PDB: 4YZM)³² have been solved previously, we were also able to examine differences between the BRD4/ligand complexes and kinase/ligand complexes for these molecules. The crystal structure of **JWG-069** (R_1 = cyclobutyl) in complex with BRD4-BD1 shows that additional hydrophobic interactions are formed by the R_1 -group and the sidechain of Trp81. Such interactions are further stabilized by Pro82 as well as the aniline tail of the compound, as was observed in the **XMD17-26** structure (R_1 = cyclopentyl, **Figure 2B and 2C**). However, such hydrophobic stacking interactions of the R_1 group are not present in the ERK5/**XMD17-26** structure, leaving the ability to inhibit the kinases effectively unaltered when compared with simple acyclic alkyl R_1 -groups. Consistent with previously published results, a gradual decrease of inhibitory activity against LRRK2 was observed upon increasing the size of the R_1 -group.^{19,20} Structural analysis of **XMD11-50** with Roco4 kinase shows that the methyl group on R_1 is accommodated by a small hydrophobic pocket formed by Leu99, Val107, and is very close to the P-loop. Larger substitutions do not fit into this space, due to a steric clash with the P-loop. However, in ERK5, the P-loop swings upward and opens this space, enabling accommodation of larger substituents (**Figure 3B**). These structures provide insight into why LRRK2 activity is changed in response to substitution at the R_1 position, whilst there is no change to ERK5 activity.

The observations i) that the N-methyl amide group of the diazopinone ring fills the hydrophobic cavity of BRD4-BD1

and ii) that the ACK probe **XMD8-87** which lacks a methyl group at this position shows much weaker inhibition of BRD4-BD1 encouraged us to explore the effect of N-methylation at the R_3 position. Four pairs of compounds (R_2 =Me/H) with different R_1 substitution were first compared (**Supplemental Table 2**). Compounds with R_2 =H show lower affinities for both BRD4 and ERK5 with the exception of ACK. The same phenomenon was observed for **XMD11-50** (LRRK2 probe), **XMD12-1** (Aurora A probe) and their pairs. These activity patterns indicate that the N-methyl amide pharmacophore is essential for both BRD4 and ERK5 binding. **JWG-112**, the hydrogen analog of the selective ERK5 inhibitor **JWG-071**, was also synthesized and tested. As expected, inhibitory activity toward both BRD4 and ERK5 decreased dramatically.

The ligand bound BRD4 structures described above show that the methoxyphenyl moiety (R_3) participates in bromo-domain binding, and the kinase structures Roco4/**XMD11-50** and ERK5/**XMD17-26** also show direct interaction between the kinase and this moiety. Therefore, we next investigated how substitution at the R_3 position modulates protein selectivity (**Table 2**). Compounds with acyclic alkyl (**JWG-046**, **JWG-049**, and **JWG-114**) or cycloalkyl substituents (**XMD17-26**, **XMD17-109**, and **JWG-047**) at the R_3 position have been tested. Increasing the size of R_3 slightly strengthened binding to BRD4, while decreasing inhibition of ERK5 and LRRK2. The structure of **JWG-047** with BRD4-BD1 revealed a small shift at the isopropoxyphenyl moiety compared to the methoxyphenyl group of **XMD17-26**, resulting in an additional structural water participating in the ligand-protein interaction and increased van de Waals interactions

Table 3. Relationship between R₁ and observed coalescence temperature, calculated half-life, and energy barrier of interconversion.

Compound ID	Corresponding parent molecule	Structure	R ₁	T _{co} (°C)	Calc t _{1/2} ^{rac} (s)	Calc ΔE _{rac} (kcal/mol)
JWG-088	XMD11-50 (LRRK2-IN-1)		Me	<25	-	-
JWG-091	JWG-048		Et	<25	-	-
JWG-082	JWG-046		<i>i</i> -Pr	47	0.07	16.3
JWG-089	JWG-069		cyclobutyl	100	2.66	18.4
JWG-090	XMD17-26		cyclopentyl	68	0.35	17.2
JWG-098	AX15836		-SO ₂ Me	120	31.0	19.9
JWG-071		As in table 2	<i>s</i> -Bu	60	0.04	15.9

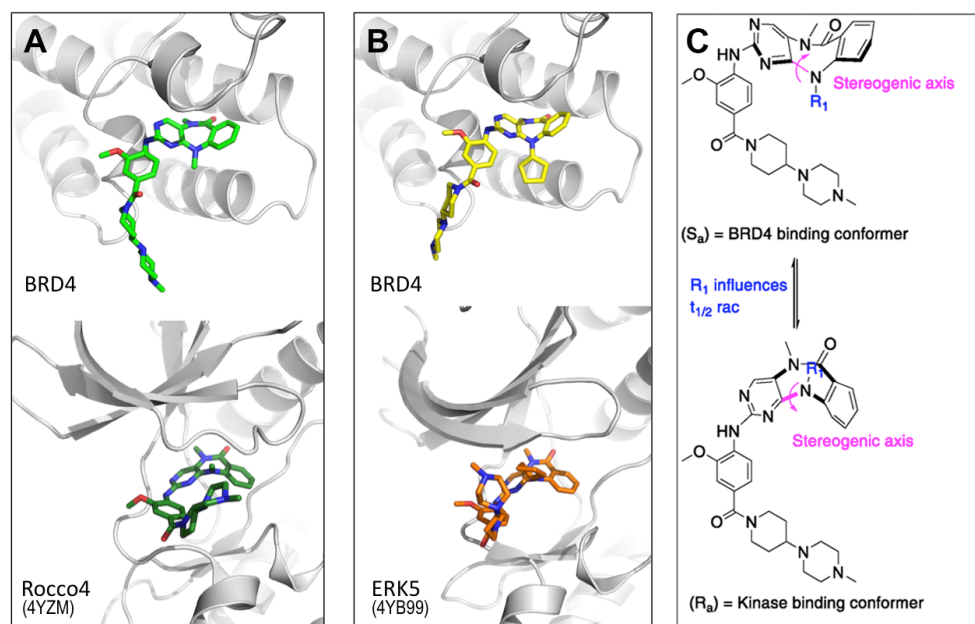


Figure 4. View showing different conformers bound to BRD4 and Kinase; (A) **XMD11-50** bound to BRD4-BD1 (upper panel) and Rocco4, pdb code 4YZM (lower panel). (B) **XMD17-26** bound to BRD4-BD1 (upper panel) and ERK5, pdb code 4B99 (lower panel). (C) Axis of chirality can rotate to generate two different conformations of the tricyclic ring system.

between the R₃ isopropyl group and Gln85 (**Figure 3C**). We did not explore R₃ substitution further because of its modest effect on binding. Ultimately, the variation of substituents at the three tested positions resulted in a dual kinase-bromodomain inhibitor **JWG-047** with BRD4 activity comparable to JQ1 (2.2 – 2.5 fold less active than JQ1).

Finally, we used the structural information to design BRD4 selective inhibitors by modifying the scaffold. Since the nitrogen atom at the 3-position of the pyrimidine is known to be critical for kinase activity by forming a key hydrogen bond with the kinase hinge region, substituting the pyrimidine for a pyridine ring should result in a compound with much lower kinase activity and this is likely to hold true across the kinome, rather than as a LRRK2/ERK5 specific effect.^{21,32} As expected, both **DFCI-2-208** and **JWG-115** lost activity against the kinase targets. However, their activity against

BRD4 also decreased 4-8 fold compared to the pyrimidine analogs **XMD11-50** and **JWG-047**, demonstrating pyrimidine core is favorable even for BRD binding (**Table 2**). **JWG-115** is a modestly potent (1 μM) BET-selective probe against the tested kinases ERK5/LRRK2.

Different atropisomeric conformers bound to BRD4 and kinases. Strikingly, when comparing kinase and BRD4 co-crystal structures, we observed that both **XMD11-50** and **XMD17-26** exhibited different conformations when bound to BRD4 than when bound to kinase targets (**Figure 4A, 4B, PDB: 4YZM and 4B99**). These conformers arise due to the axial chirality about the C-N bond in the rotationally hindered 7-membered ring (**Figure 4C**). In the kinase structures the (R_a) conformer is observed, whereas in the BRD4 structures solved here the (S_a) conformer is observed.

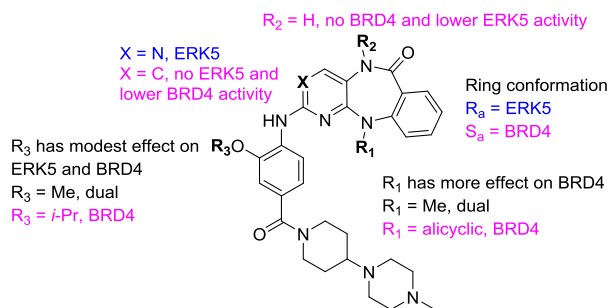


Figure 5. SAR rules for benzo[e]pyri(mi)do-[5,4-b]diazepine-6(11H)-one activity against BRD4 and ERK5 targets.

As we did not observe separation of entries 1 – 6, **Table 2**, by chiral HPLC separation, we determined $t_{1/2}^{\text{rac}}$ using NMR spectroscopy, in order to characterize whether these molecules exist as conformers or separable atropisomers. When the half-life ($t_{1/2}$) for interconversion of the two conformations is greater than 1000 seconds at room temperature, which corresponds to an interconversion energy barrier greater than 20 kcal/mol, the molecules exist as a mixture of two distinct atropisomers and each atropisomer can, in theory, be isolated.^{33,34} In this case, each atropisomer should be evaluated separately for its ability to bind to BRD4, ERK5 and LRRK2. We anticipated the $t_{1/2}$ in this series to be influenced by the steric bulk of R_1 . In order to generate diastereomers that exhibit distinct ^1H NMR resonances which would enable characterization of the $t_{1/2}$ of racemization using variable temperature ^1H NMR experiments we synthesized the corresponding (-)-menthol derivatives of R_1 variants. Considering menthol and methyl-4-(piperidine-4-yl) piperazine moieties at the tail position are likely to have little effect on the 7-membered ring conformation, we hypothesized that the parent molecules have similar interconversion temperatures as (-)-menthol derivatives. **JWG-071** ($R_1 = \text{sec-butyl}$) contains a stereocenter and the potential for four diastereomers. In this molecule we could directly observe two sets of NMR signals, therefore we could measure the coalescence temperature directly (60 °C) without needing to resort to the preparation of chiral menthol esters.

At room temperature, **JWG-088** and **JWG-091** exhibited only a single set of NMR resonances indicating that they are achiral compounds whose conformers interconvert rapidly. Once R_1 was increased, the compounds exhibited two sets of resonances with equal abundance (**JWG-082**, **JWG-089**, and **JWG-090**). Hence, we performed variable temperature ^1H NMR experiments from 25 °C to 120 °C in DMSO- d_6 (Supplemental Spectra) and observed that the coalescence temperatures of isopropyl, cyclobutyl, and cyclopentyl analogs were 47 °C, 100 °C and 68 °C respectively (**Table 3** and Supplemental Spectra). During the course of this work, another group reported modification of **XMD17-109** to generate **AX15836** that possess excellent ERK5 activity and selectivity against BRD4.²⁶ We independently synthesized and confirmed the activity and selectivity of this inhibitor (**Table 2**). We also synthesized the corresponding menthol ester **JWG-098** ($R_1 = \text{methylsulfonyl}$) and observed its coalescence temperature to be 120 °C (**Table 3**).

We next calculated the half-lives and energy barriers for interconversion of the compounds. As we expected, the R_1 substituent affected the energy barrier and rate of interconversion between conformers, and this conclusion was supported by

quantum mechanical analysis of the ground and transition states of the conformers of **XMD11-50** and **XMD17-26** (**Table 3**, **Supplemental Figure 5**). Nevertheless, all analogs had energy barriers lower than 20 kcal/mol, indicating that these analogs interconverted with half-lives measured in seconds and can therefore not be separated at room temperature.

In the absence of separable atropisomers, we used docking studies to explore the observed isomer preferences of kinases and bromodomains. Using the dual kinase-bromodomain targeting analogs **XMD11-50** and **XMD17-26**, the R_a and S_a conformations of each compound were frozen and docked into apo BRD4 bromodomain and ERK5 kinase domain structures. For both compounds, low energy solutions were found for the S_a conformers docked into BRD4, but no solutions were found for the R_a conformer. Similarly, low energy solutions were found for the R_a conformer docked into ERK5, but no solutions were found for the S_a conformer, indicating that the observed preferences in crystallography are due to differing binding affinities of the conformers for each target (**Supplemental Figure 6**). We anticipate that compounds that introduce further steric constraints to the diazepine core might possess atropisomers that could be separated. In contrast to **JWG-071**, **JWG-112** displays only one set of NMR resonances at room temperature, suggesting substitution at R_2 position also increases steric hindrance and can be a further modification spot. Our computational analysis indicates that separable atropisomers may display kinase selectivity (R_a) or BRD selectivity (S_a) dependent on their chirality.

Conclusions. In this paper, we identify a new class of dual kinase-bromodomain inhibitors with a shared hetero-tricyclic core. Through SAR studies and complementary structural studies, we defined a blueprint for tuning in or out kinase or bromodomain activity (**Figure 5**). This resulted in identification of an ERK5 selective chemical probe (**JWG-071**) and a BRD4 selective probe (**JWG-115**) as well as inhibitors with rationally designed polypharmacology (**JWG-047**, **JWG-069**). We also observed different conformational isomers in bromodomain vs kinase X-ray structures, leading to investigation of the atropisomeric properties of this scaffold. Atropisomerism has previously been exploited to improve the subfamily selectivity of kinase inhibitors.³⁵ In this work we report the first example of different protein target classes distinguishing between atropisomeric conformers. Since the 7-membered diazepine ring is widely used in drug development and exists in natural products³⁶, this newly discovered contribution of atropisomers to protein target selectivity is a highly relevant topic warranting further investigation. Future work will focus on synthesis of enantiomerically pure analogs with slower interconversion rates to evaluate the binding ability to BRD4 and kinases of each isomer.

METHODS

Protein Preparation. The first bromodomain of Brd4 (BRD4-BD1, residues 42-168) was subcloned into a modified pET-15b(+) vector with an N-terminal His₆ tag followed by a Tobacco Etch Virus cleavage site. The encoded protein was expressed in the E. coli BL21(DE3) strain. E. coli cells transformed with the vector were grown 4 hours at 37 °C to an OD600 of 1.0, in 1 liter LB media containing ampicillin (0.1 mg/ml). After 0.1 mM IPTG induction at 20 °C, cells were cultured overnight, and collected by centrifugation at 4,000 g. The pellet was suspended in 40 ml lysis buffer containing 50 mM HEPES, pH 7.4, 500 mM NaCl, 5 mM β -

mercaptoethanol, and 1 mM PMSF. Cells were lysed on ice by sonication and cell debris was precipitated by centrifugation at 15,000 g for 30 minutes. BRD4-BD1 was purified by affinity chromatography on an Ni-NTA agarose column (Qiagen), using an elution buffer of 50 mM HEPES, pH 7.4, 500 mM NaCl, 5 mM β -mercaptoethanol, and 250 mM of imidazole. After overnight TEV cleavage of the His₆-tag, the cleaved tag was captured on affinity resin, and BRD4-BD1 was then purified to homogeneity by gel filtration before concentration to roughly 15 mg/ml in storage buffer (25mM HEPES, pH 7.4, and 150 mM NaCl).

Bromodomain BRD4-1 AlphaScreen binding assay in Dana-Farber Cancer Institute. Assays were performed with minor modifications from the manufacturer's protocol (Perkin Elmer, USA). All reagents were diluted in AlphaScreenTM buffer (50 mM HEPES, 150 mM NaCl, 0.01% v/v Tween-20, 0.1% w/v BSA, pH = 7.4). After addition of Alpha beads to master solutions, all subsequent steps were performed under low light conditions. A 2x solution of components with final concentrations of His-Brd4(1) at 0.020 μ M, Ni-coated Acceptor Bead at 10 μ g/ml, and biotinylated-(+)-JQ1 at 0.010 μ M were added in 10 μ L to 384-well plates (AlphaPlate-384, PerkinElmer) using an EL406 liquid handler (Biotek, USA). Plates were spun down at 1000 rpm. A 10-point 1: 3 serial dilution of compounds in DMSO was prepared at 200x the final concentration. 100 nL of compound from these stock plates were added by pin transfer using a Janus Workstation (PerkinElmer). A 2x solution of streptavidin-coated donor beads with a final concentration of 10 μ g/ml was added in a 10 μ L volume. The plates were spun down again at 1000 rpm and sealed with foil to prevent light exposure and evaporation. The plates were then incubated at room temperature for 1 h and read on an Envision 2104 (PerkinElmer) using the manufacturer's protocol. IC₅₀ values were calculated using a 4-parameter logistic curve in Prism 6 (GraphPad Software, USA) after normalization to DMSO-treated negative control wells (0.2% DMSO, v/v).

Bromodomain BRD4-1 AlphaScreen binding assay in University of Oxford. Assays were performed as described previously with minor modifications from the manufacturer's protocol (PerkinElmer, USA). All reagents were diluted in 25 mM HEPES, 100 mM NaCl, 0.1 % BSA, pH 7.4 and 0.05 % CHAPS and allowed to equilibrate to room temperature prior to addition to plates. A 11-point 1:2.0 serial dilution of the ligands was prepared on low-volume 384-well plates (ProxiPlateTM-384 Plus, PerkinElmer, USA) using LabCyte Eco liquid handler. Plates filled with 5 μ L of the assay buffer followed by 7 μ L of biotinylated peptide [H-YSGRGGKacGGKacGLGKacGGAKacRHRK(Biotin)-OH and His-tagged protein to achieve final assay concentrations of 25 nM. Plates were sealed and incubated for a further 60 minutes, before the addition of 8 μ L of the mixture of streptavidin-coated donor beads (12.5 μ g/ml) and nickel chelate acceptor beads (12.5 μ g/ml) under low light conditions. Plates were foil-sealed to protect from light, incubated at room temperature for 60 minutes and read on a PHERAstar FS plate reader (BMG Labtech, Germany) using an AlphaScreen 680 excitation/570 emission filter set. IC₅₀ values were calculated in Prism 6 (GraphPad Software, USA) after normalization against corresponding DMSO controls and are given as the final concentration of compound in the 20 μ L reaction volume.

Isothermal Titration Calorimetry. Experiments were performed using a MicroCal ITC200 calorimeter (GE

Healthcare). All experiments were carried out at 25 °C with 1000 RPM stirring speed, in a buffer containing 25mM HEPES pH7.5 and 100 mM NaCl. The injection syringe was loaded with a solution of the protein sample at 200 μ M concentration and the cell was filled with compound at 20 μ M concentration. Single binding site model in Origin software (OriginLab, Northampton MA USA) was employed to calculate dissociation constants and thermodynamic parameters.

Protein Stability Assay. Differential scanning fluorimetry (DSF) was used to measure stabilization of BRD4-BD1 at 2 μ M concentration in the presence of 10 μ M compound in a volume of 20 μ L. SYPRO Orange (Molecular Probes) was included (diluted 1:1000) as the fluorescence probe, with excitation and emission wavelength set to 465nm and 590nm, respectively. Fluorescence measurements were taken regularly over a thermal gradient from 25 °C to 95 °C using a ramp rate of 3 °C per minute. The data were plotted using non-linear least squares fitting, and temperature shifts were calculated as the difference between the transition midpoints of the protein with and without compounds.

ERK5 kinase activity in vitro assay. A 40 μ L reaction mixture was prepared containing 200 ng of pure active ERK5 and the indicated amount of inhibitor in 50 mM Tris-HCl, pH 7.5, 0.1 mM EGTA, 1 mM 2-mercaptoethanol. The reaction was initiated by adding 10 mM magnesium acetate, and 50 μ M [γ -³²P]-ATP (500 cpm/pmol) and 200 μ M PIMtide (ARKKRRHPSGPPTA) as substrates. Assays were carried out for 20 min at 30 °C, terminated by applying the reaction mixture onto p81 paper and the incorporated radioactivity measured as described previously. The expression and purification of ERK5 was carried out as described previously.³⁷

LRRK2 kinase activity in vitro assay. An *in vitro* assay of LRRK2 kinase activity was performed in Adapta kinase assay format at Thermo Fisher Scientific (Madison, WI) using the SelectScreen Kinase Profiling Service. All protocols are available from the Thermo Fisher Scientific website.

797 NMC Cell Viability Assay. Cells were plated in a 96-well plate at a density of 5,000 cells/well and incubated for 3 days in the presence of various concentration of compounds or DMSO. Relative cell numbers were determined in 6 replicates using Cell Titer Glo (Promega, Madison, WI) according to the manufacturer's instructions.

Cellular assay of ERK5. Human HeLa cells were serum starved overnight followed by treatment with the indicated inhibitor for one hour. Cells were then stimulated with EGF (50 ng/mL) for 20 min and harvested in RIPA buffer (1X PBS, 1% NP40, 0.5% sodium deoxycholate, 0.1% SDS, 0.1 mg/ml PMSF and 1mM sodium orthovanadate). Proteins from total cell lysates were resolved by 6% sodium dodecyl sulfate (SDS)-polyacrylamide gel electrophoresis (PAGE), transferred to nitrocellulose membrane, blocked in 5% nonfat milk, and blotted with anti-ERK5 antibody (Cell Signaling Technology, Boston, MA). Active ERK5 activity was calculated by monitoring the amount of retarded, autophosphorylated band in the immunoblots, as described elsewhere.

Crystallization and Data Collection. BRD4-BD1 complexes were crystallized using the hanging drop vapor diffusion method at room temperature, using either co-crystallization or soaking methods. For soaking experiments, inhibitor-free crystals were first obtained in a drop with equal volumes of BD1 at 4 mg/ml and a precipitant solution containing 100mM sodium nitrate, 5% ethylene glycol, and 18%

(w/v) PEG3350, as precipitant. Rod-like crystals obtained in 10 days were transferred and soaked in the same crystallization buffer pulsing compounds at 0.5 mM concentration for 5-7 days. For co-crystallization experiments, protein was first incubated with compounds at molar ratio of 1:3 and then mixed with the same precipitant solution as in soaking experiments. For data collection, a single crystal was picked and flash-frozen with a precipitant solution containing 20% (v/v) glycerol. Diffraction data for each complex were collected from a flash-cooled crystal at 100 °K using the NE-CAT 24ID-C or 24ID-E beam lines at Argonne National Laboratory. Data were processed, integrated, and scaled using HKL2000 (Otwinowski, Z., and Minor, W. (1997)).

Structure determination and refinement. Structures of BRD4-BD1 complexes were solved by molecular replacement (MR) in Phenix³⁸ using the BD1-UMB32 structure (PDB 4WIV) as a search model. Structure refinement was carried out using conjugate-gradient energy minimization, torsion-constrained molecular dynamics simulated annealing, group B factor refinement, and individual B factor refinement protocols in Phenix with 5% of the reflections omitted for free R factor calculation. Electron density peaks above 3σ in difference Fourier maps were assigned to water molecules in later refinement stages if they had reasonable geometry in relation to hydrogen bond donors or acceptors and their B-factors did not rise above 50 Å² during subsequent refinement. Model building was performed in Coot guided by σ A-weighted 2Fo-Fc and Fo-Fc maps and composite omit maps.

Kinome Profiling. Kinome profiling was performed using KinomeScan ScanMAX at compound concentration of 1 μ M. Data was reported in Supplemental data. Protocols are available from DiscoverX.

ASSOCIATED CONTENT

Supporting Information

The Supporting Information is available free of charge on the ACS Publications website.

Experimental procedures, supporting figures, supporting tables; kinase selectivity profile of JWG-071; and variable temperature 1H NMR spectra (PDF)

AUTHOR INFORMATION

Corresponding Author

* E-mail: Xiang_Xu@hms.harvard.edu

* E-mail: Nathanael_Gray@dfci.harvard.edu

Funding Sources

This work was supported by the NIH LINCS Program grant U54HL127365 (to N. S. Gray and J. Wang), NIH P50 GM107618 (to X. Xu and S. C. Blacklow), the Spanish Ministerio de Economía y Competitividad (MINECO) grant SAF2015-60268R (to J.M. Lizcano) and co-funded by Fondo Europeo de Desarrollo Regional (FEDER) funds. D.L. Buckley was supported as a Merck Fellow of Damon Runyon Cancer Research Foundation (DRG-2196-14).

ACKNOWLEDGMENTS

We thank P Cohen for helpful discussion. We also thank E Meigas for technical support.

REFERENCES

- (1) Filippakopoulos, P.; Picaud, S.; Mangos, M.; Keates, T.; Lambert, J.-P.; Barseyte-Lovejoy, D.; Felletar, I.; Volkmer, R.; Müller, S.; Pawson, T.; Gingras, A.-C.; Arrowsmith, Cheryl H.; Knapp, S. *Cell* **2012**, *149*, 214.
- (2) Winter, G. E.; Mayer, A.; Buckley, D. L.; Erb, M. A.; Roderick, J. E.; Vittori, S.; Reyes, J. M.; di Iulio, J.; Souza, A.; Ott, C. J.; Roberts, J. M.; Zeid, R.; Scott, T. G.; Paulk, J.; Lachance, K.; Olson, C. M.; Dastjerdi, S.; Bauer, S.; Lin, C. Y.; Gray, N. S.; Kelliher, M. A.; Churchman, L. S.; Bradner, J. E. *Mol Cell* **2017**.
- (3) Yang, Z.; Yik, J. H. N.; Chen, R.; He, N.; Jang, M. K.; Ozato, K.; Zhou, Q. *Molecular Cell* **2005**, *19*, 535.
- (4) Itzen, F.; Greifenberg, A. K.; Bosken, C. A.; Geyer, M. *Nucleic acids research* **2014**, *42*, 7577.
- (5) Jonkers, I.; Lis, J. T. *Nature reviews. Molecular cell biology* **2015**, *16*, 167.
- (6) Chapuy, B.; McKeown, M. R.; Lin, C. Y.; Monti, S.; Roemer, M. G.; Qi, J.; Rahl, P. B.; Sun, H. H.; Yeda, K. T.; Doench, J. G.; Reichert, E.; Kung, A. L.; Rodig, S. J.; Young, R. A.; Shipp, M. A.; Bradner, J. E. *Cancer Cell* **2013**, *24*, 777.
- (7) Ott, C. J.; Kopp, N.; Bird, L.; Paranal, R. M.; Qi, J.; Bowman, T.; Rodig, S. J.; Kung, A. L.; Bradner, J. E.; Weinstock, D. M. *Blood* **2012**, *120*, 2843.
- (8) Loven, J.; Hoke, H. A.; Lin, C. Y.; Lau, A.; Orlando, D. A.; Vakoc, C. R.; Bradner, J. E.; Lee, T. I.; Young, R. A. *Cell* **2013**, *153*, 320.
- (9) Tanaka, M.; Roberts, J. M.; Qi, J.; Bradner, J. E. *Pharmaceutical patent analyst* **2015**, *4*, 261.
- (10) Fiskus, W.; Sharma, S.; Qi, J.; Shah, B.; Devaraj, S. G.; Leveque, C.; Portier, B. P.; Iyer, S.; Bradner, J. E.; Bhalla, K. N. *Molecular cancer therapeutics* **2014**, *13*, 2315.
- (11) Lee, D. H.; Qi, J.; Bradner, J. E.; Said, J. W.; Doan, N. B.; Forscher, C.; Yang, H.; Koeffler, H. P. *International journal of cancer* **2015**, *136*, 2055.
- (12) Shu, S.; Lin, C. Y.; He, H. H.; Witwicki, R. M.; Tabassum, D. P.; Roberts, J. M.; Janiszewska, M.; Huh, S. J.; Liang, Y.; Ryan, J.; Doherty, E.; Mohammed, H.; Guo, H.; Stover, D. G.; Ekram, M. B.; Peluffo, G.; Brown, J.; D'Santos, C.; Krop, I. E.; Dillon, D.; McKeown, M.; Ott, C.; Qi, J.; Ni, M.; Rao, P. K.; Duarte, M.; Wu, S. Y.; Chiang, C. M.; Anders, L.; Young, R. A.; Winer, E. P.; Letai, A.; Barry, W. T.; Carroll, J. S.; Long, H. W.; Brown, M.; Liu, X. S.; Meyer, C. A.; Bradner, J. E.; Polyak, K. *Nature* **2016**, *529*, 413.
- (13) Ember, S. W.; Zhu, J. Y.; Olesen, S. H.; Martin, M. P.; Becker, A.; Berndt, N.; Georg, G. I.; Schonbrunn, E. *ACS chemical biology* **2014**, *9*, 1160.
- (14) Ciceri, P.; Muller, S.; O'Mahony, A.; Fedorov, O.; Filippakopoulos, P.; Hunt, J. P.; Lasater, E. A.; Pallares, G.; Picaud, S.; Wells, C.; Martin, S.; Wodicka, L. M.; Shah, N. P.; Treiber, D. K.; Knapp, S. *Nature chemical biology* **2014**, *10*, 305.
- (15) Chen, L.; Yap, J. L.; Yoshioka, M.; Lanning, M. E.; Fountain, R. N.; Raje, M.; Scheenstra, J. A.; Strovel, J. W.; Fletcher, S. *ACS medicinal chemistry letters* **2015**, *6*, 764.
- (16) Koblan, L. W.; Buckley, D. L.; Ott, C. J.; Fitzgerald, M. E.; Ember, S. W.; Zhu, J. Y.; Liu, S.; Roberts, J. M.; Remillard, D.; Vittori, S.; Zhang, W.; Schonbrunn, E.; Bradner, J. E. *ChemMedChem* **2016**, *11*, 2575.
- (17) Miduturu, C. V.; Deng, X.; Kwiatkowski, N.; Yang, W.; Brault, L.; Filippakopoulos, P.; Chung, E.; Yang, Q.; Schwaller, J.; Knapp, S.; King, R. W.; Lee, J. D.; Herrgard, S.; Zarrinkar, P.; Gray, N. S. *Chemistry & biology* **2011**, *18*, 868.
- (18) Roberts, J. M.; Bradner, J. E. *Current protocols in chemical biology* **2015**, *7*, 263.

- (19) Deng, X.; Dzamko, N.; Prescott, A.; Davies, P.; Liu, Q.; Yang, Q.; Lee, J. D.; Patricelli, M. P.; Nomanbhoy, T. K.; Alessi, D. R.; Gray, N. S. *Nature chemical biology* **2011**, *7*, 203.
- (20) Deng, X.; Elkins, J. M.; Zhang, J.; Yang, Q.; Erazo, T.; Gomez, N.; Choi, H. G.; Wang, J.; Dzamko, N.; Lee, J. D.; Sim, T.; Kim, N.; Alessi, D. R.; Lizcano, J. M.; Knapp, S.; Gray, N. S. *Eur J Med Chem* **2013**, *70*, 758.
- (21) Elkins, J. M.; Wang, J.; Deng, X.; Pattison, M. J.; Arthur, J. S.; Erazo, T.; Gomez, N.; Lizcano, J. M.; Gray, N. S.; Knapp, S. *Journal of medicinal chemistry* **2013**, *56*, 4413.
- (22) Yang, Q.; Deng, X.; Lu, B.; Cameron, M.; Fearn, C.; Patricelli, M. P.; Yates Iii, J. R.; Gray, N. S.; Lee, J.-D. *Cancer Cell* **2010**, *18*, 258.
- (23) Kwiatkowski, N.; Deng, X.; Wang, J.; Tan, L.; Villa, F.; Santaguida, S.; Huang, H. C.; Mitchison, T.; Musacchio, A.; Gray, N. *ACS chemical biology* **2012**, *7*, 185.
- (24) Kwiatkowski, N.; Jelluma, N.; Filippakopoulos, P.; Soundararajan, M.; Manak, M. S.; Kwon, M.; Choi, H. G.; Sim, T.; Deveraux, Q. L.; Rottmann, S.; Pellman, D.; Shah, J. V.; Kops, G. J.; Knapp, S.; Gray, N. S. *Nature chemical biology* **2010**, *6*, 359.
- (25) Sureban, S. M.; May, R.; Weygant, N.; Qu, D.; Chandrakesan, P.; Bannerman-Menson, E.; Ali, N.; Pantazis, P.; Westphalen, C. B.; Wang, T. C.; Houchen, C. W. *Cancer letters* **2014**, *351*, 151.
- (26) Lin, E. C.; Amantea, C. M.; Nomanbhoy, T. K.; Weissig, H.; Ishiyama, J.; Hu, Y.; Sidique, S.; Li, B.; Kozarich, J. W.; Rosenblum, J. S. *Proceedings of the National Academy of Sciences of the United States of America* **2016**, *113*, 11865.
- (27) Montero, J. C.; Ocana, A.; Abad, M.; Ortiz-Ruiz, M. J.; Pandiella, A.; Esparis-Ogando, A. *PloS one* **2009**, *4*, e5565.
- (28) Sticht, C.; Freier, K.; Knopfle, K.; Flechtenmacher, C.; Pungs, S.; Hofele, C.; Hahn, M.; Joos, S.; Lichter, P. *Neoplasia* **2008**, *10*, 462.
- (29) Hayashi, M.; Fearn, C.; Eliceiri, B.; Yang, Y.; Lee, J. D. *Cancer research* **2005**, *65*, 7699.
- (30) Vidler, L. R.; Filippakopoulos, P.; Fedorov, O.; Picaud, S.; Martin, S.; Tomsett, M.; Woodward, H.; Brown, N.; Knapp, S.; Hoelder, S. *Journal of medicinal chemistry* **2013**, *56*, 8073.
- (31) French, C. A.; Miyoshi, I.; Kubonishi, I.; Grier, H. E.; Perez-Atayde, A. R.; Fletcher, J. A. *Cancer research* **2003**, *63*, 304.
- (32) Gilsbach, B. K.; Messias, A. C.; Ito, G.; Sattler, M.; Alessi, D. R.; Wittinghofer, A.; Kortholt, A. *Journal of medicinal chemistry* **2015**, *58*, 3751.
- (33) Laplante, S. R.; L, D. F.; Fandrick, K. R.; Fandrick, D. R.; Hucce, O.; Kemper, R.; Miller, S. P.; Edwards, P. J. *Journal of medicinal chemistry* **2011**, *54*, 7005.
- (34) LaPlante, S. R.; Edwards, P. J.; Fader, L. D.; Jakalian, A.; Hucce, O. *ChemMedChem* **2011**, *6*, 505.
- (35) Smith, D. E.; Marquez, I.; Lokensgard, M. E.; Rheingold, A. L.; Hecht, D. A.; Gustafson, J. L. *Angewandte Chemie (International ed. in English)* **2015**, *54*, 11754.
- (36) Smyth, J. E.; Butler, N. M.; Keller, P. A. *Nat Prod Rep* **2015**, *32*, 1562.
- (37) Erazo, T.; Moreno, A.; Ruiz-Babot, G.; Rodriguez-Asiain, A.; Morrice, N. A.; Espadamala, J.; Bayascas, J. R.; Gomez, N.; Lizcano, J. M. *Molecular and cellular biology* **2013**, *33*, 1671.
- (38) Adams, P. D.; Afonine, P. V.; Bunkoczi, G.; Chen, V. B.; Davis, I. W.; Echols, N.; Headd, J. J.; Hung, L. W.;
- Kapral, G. J.; Grosse-Kunstleve, R. W.; McCoy, A. J.; Moriarty, N. W.; Oeffner, R.; Read, R. J.; Richardson, D. C.; Richardson, J. S.; Terwilliger, T. C.; Zwart, P. H. *Acta crystallographica. Section D, Biological crystallography* **2010**, *66*, 213.
-